

## DELINEATION OF POTENTIAL MINERAL ZONES USING INTEGRATED AEROMAGNETIC AND AEROGRAVITY DATA OVER PART OF ZAMFARA STATE, NORTH WESTERN NIGERIA

\*<sup>1</sup>Ibrahim Sani, <sup>2</sup>Jamaluddeen S. Shehu and <sup>3</sup>Faiza Ahmed

<sup>1</sup>Department of Physics, Federal University Gusau, Nigeria

<sup>2</sup>Department of Physics, Bayero University Kano, Nigeria

\*Corresponding authors' email: [ibrahimsani@fugusau.edu.ng](mailto:ibrahimsani@fugusau.edu.ng) Phone: +2348139037494

### ABSTRACT

This study aims to delineate potential mineral-bearing zones in Zamfara State using integrated aeromagnetic and aerogravity data interpretation. Acquired aeromagnetic and aerogravity data of part of Zamfara State that lies between latitudes 11° 30' 0" N and 12° 30' 0" N, and longitudes 6° 00' 0" E and 7° 00' 0" E were used to delineate structures that may host minerals in the study area. The area forms part of the northern Nigerian basement complex with granite, migmatite, biotite, gneiss, diorite, medium course grained, and migmatite augen gneiss as host rocks in the region. Advanced filtering techniques—FVD, AS, and SPI—were applied to enhance structural features, estimate source depths, and identify lineaments indicative of mineralization. The data were subjected to various filtering techniques such as first vertical derivative (FVD), analytical signal (AS), source parameter imaging (SPI) and lineaments analysis. The FVD maps for both the data enhance shallow anomalies ranges from -170nT/m to 0.166nT/m and -66.8mgal/m to 74.4mgal/m. The AS maps indicate magnetic anomaly edges and their source positions with values 0.088nT/m to 0.4417nT/m and 6.5mgal/m to 118.4mgal/m. Anomalies indicating possible mineral zones were observed at depths ranging from approximately 35 m to over 5,000 m. SPI maps revealed the depth to the anomalous sources ranges from 35.0m to 357.0m and 260.8m to 5192.5m. Lineaments analysis determined faults and fractures of the rocks within the study area. The integrated analysis delineated several structurally controlled zones near Lugga, Maru, Yantauri, and Tudun Wada with strong geophysical signatures consistent with mineralization. "The isolated the potential mineral zones are 12.450N to 12.060 N and 6.440E to 6.250E, 12.460N to 12.310N and 6.730E to 6.890E, 11.770N to 11.880N and 6.590E to 6.460E corresponding to Lugga, Maru, Kukulai, Gidan Awala, Yantauri, Dutsin Kura, Ungwan Kane Mazanya and Tudun Wada areas. Integrating the data provides a clear resolution that revealed complex geologic structures. These findings provide a geophysical basis for targeted mineral exploration, which could support economic development initiatives in the region. Delineating mineral zones can ease mining process, create a productive environment for business opportunities, and boost the nation's economy.

**Keywords:** Aeromagnetic, Aerogravity, Analytical signal, First Vertical Derivative, Oasis Montaj

### INTRODUCTION

Minerals are of importance to the economy of a nation if discovered and harnessed, as this will create a productive environment for business opportunities, boost the nation's economy and provide raw materials for industrial uses that might in turn reduce the level of unemployment there by eradicating poverty (Adewumi & Salako, 2018). Exploitation of mineral resources has assumed prime importance in several developing countries including Nigeria. Nigeria is endowed with abundant mineral resources, which have contributed immensely to the national wealth with associated socioeconomic benefits. Mineral resources are of important source of wealth for a nation but before they are harnessed, they have to pass through the stages of exploration, mining and processing (Adekoya, 2003). Zamfara as a state has been blessed with mineral resources such as gold, iron ore, chamovite, granite, clay, limestone, quartz and kaolin. However, none of these mineral resources have been fully exploited which will enable them to become major contributors to Nigerian economy. Owing to the effort by the artisanal miners many of the minerals have been discovered. However, the artisanal miners use local methods of exploration which make it difficult to locate zones containing minerals in the area (Augie & Ridwan, 2021). The use of trial and error method for minerals exploration does not yield a better result of locating mineral zones in the area rather create environmental degradation which resulted from abandoned pit holes and trenches. To locate potential mineral zones,

qualitative interpretation of aeromagnetic and aerogravity data was employed in order to save the environment from deteriorating. As part of the effort made by zamfara state government in transforming the state through industrial revolution, minerals play a very magnificent role in transforming industries and societies in different ways such as energy source, raw materials, technological advancement, economic growth and infrastructure development.

Geophysical techniques plays an important role in mineral investigation, which ranges from structure delineations to detect possible areas of ore deposits, since minerals are structurally controlled (Priscillia et al., 2021). Gravity and magnetic data are important in locating features that are seismically less easy to recognize such as strike-slip faults, regional discontinuities, dykes and basement surface (Fairhead, 2009). Geophysical techniques (aeromagnetic and aerogravity) were used since terrestrial measurement of data is limited to only accessible areas. Areas that are not easily accessible due to lack of access routes, insecurity and cost etc. are found unfavorable for terrestrial measurement of data. Aeromagnetic exploration is often times carried out to investigate the distributions of bedrock lithologies and structures (Priscillia et al., 2021). Aeromagnetic data are consistently used for economic interest targeting and geological mapping. Besides solving problems that are concerned with the basement, the method has become a useful tool in exploring minerals, hydrocarbons occurrence, groundwater investigations, and geothermal potentials

(Adagunodo et al., 2015). The magnetic method measures the variation in the magnetic field of the materials above the curie depth that is usually produced as the results of remnant and induced magnetization compared with the mineralized bodies and the host rock (Augie & Ologe, 2020). Most subsurface mineralized bodies are associated with the deformation activities, the interpretation of aeromagnetic data can aid the visualization of subsurface geological features that are covered by over burden that serves as the search of conduit for mineralized bodies (Sani et al., 2019). The airborne gravity value is the gravity value at a certain height. The data comes from measuring the value of the gravitational field in the air using aircraft vehicles with a wide range of measurements covering various areas that are difficult to reach by land, such as forests, valleys, and mountains (Syafnur et al., 2019). Airborne gravity also analyzes geological lineament and basement depth (Indriyani et al., 2023).

Gravity method is a geophysical investigation method that is used to identify and describe rocks lithology, geological structures and subsurface structures depending on varied earth's gravity that is caused by difference in various rocks' density. Both gravity and magnetic methods have a great deal in common and an interface for geological interpretation can be established between them. They are both extensively used as reconnaissance tools in oil exploration, mineral exploration as well as deep crustal studies (Ibim et al., 2025). Although different authors such as Augie and Ridwan, (2021) and Dalhatu et al., (2022) conducted some researches to locate

potential mineral zones as well as subsurface investigation in the study area employing aeromagnetic data. Aeromagnetic anomaly map captures only magnetic response from the magnetic bodies within the subsurface resulting in limited resolution., shallow resolution, inability to resolve structural complexity in areas with complex geology (Jamaludin et al., 2021). Ibim et al., (2025) conducted a research and successfully delineated subterranean structural features of the basement complex, Imo river basin, southeastern Nigeria using integrated magnetic and gravity data. This study aims to address this limitation by integrating aeromagnetic with aerogravity data that captures density contrast within the subsurface and provided more comprehensive geological insight as different geophysical methods complement each other's strengths and weaknesses. This work provides a more comprehensive delineation of potential mineral zones through an integrated interpretation of high-resolution aeromagnetic and aerogravity data.

### Location and Geology of the Study Area

The study area lies between latitudes 11°30'0"n to 12°30'0"n, and longitudes 6°00'0"e to 7°00'0"e. These areas cover; Gusau, Tsafe, Maru and Dan Gulbi local government (figure 1). The area is central part of Zamfara Nigeria that forms part of the northern Nigerian basement complex (figure 2). The kind of rocks forming minerals there are; granite, migmatite, biotite, gneiss, diorite, medium course grained, and migmatite augen gneiss (Augie & Ridwan, 2021)

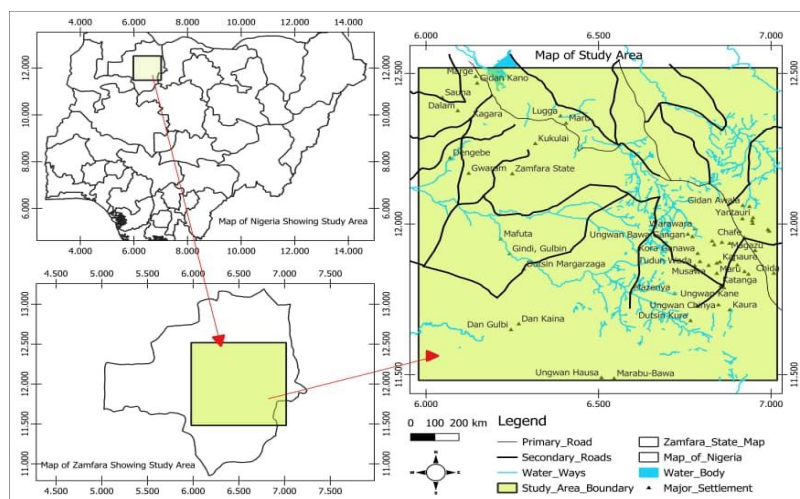


Figure 1: Location of the Study Area

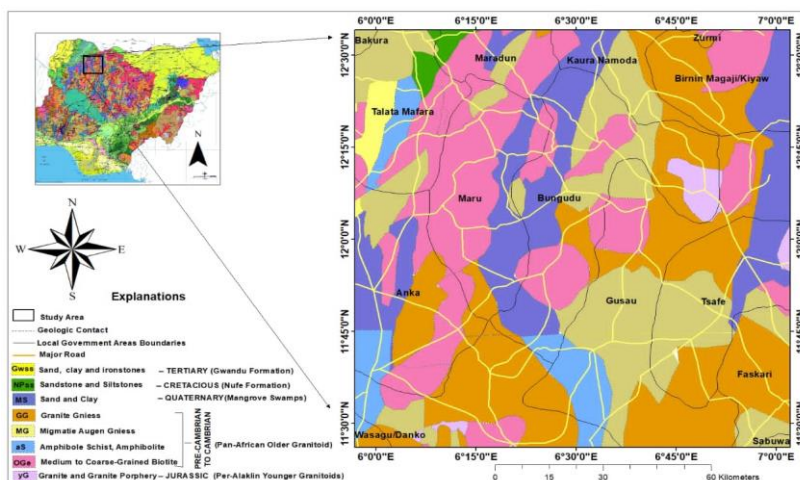


Figure 2: Geological Map of the Study Area (NGSA,2006)

## MATERIALS AND METHODS

### Materials

Four high-resolution aeromagnetic maps over part of Zamfara state were acquired which include Maru (sheet 53), Gusau (sheet 54), Dan Gulbi (sheet 76) and Tsafe (sheet 77). These maps were obtained as part of the nationwide airborne survey carried out by Fugro and sponsored by the Nigerian Geological Survey Agency (NGSA) in the year 2009. The data were obtained at an altitude of 100 m along a flight line spacing of 500 m oriented in nw-se and a tie line spacing of 2000 m. The maps are on a scale of 1:100,000 and half-degree sheets contoured mostly at 10nT intervals. The geomagnetic gradient was removed from the data using the international geomagnetic reference field (IGRF). The actual magnetic intensity value of 33,000 nt which was reduced for handling must be added to the value of magnetic intensity at any point so as to get the actual value of the magnetic intensity (using IGRF model 2007).

The aerogravity data were obtained from Bureau Gravimetric International (BGI) through the <http://bgi.obs-mip.fr/dataproducts/gravity-databases/land-gravity-datas/>.

The survey was carried out in conjunction with IAG international gravity field service. The main job of bgi is to gather all gravity measurements (relative or absolute) and pertinent information about the gravity field of the earth on a worldwide basis, compile and authenticate them, and store them in a computerized database in order to redistribute them on request to multiple users for scientific applications. BGI produces the most precise information available on the earth's gravity field at short wavelengths today, and it is very complementary to airborne and satellite gravity measurements. The satellite gravity data were recorded in digital layout (x, y, and z). X, y, and z represent the longitude, latitude, and bouguer anomaly (density contrast) of the study area, respectively. Corrections such as Bouguer, drift, earth-tide, elevation, terrain, and latitude were all applied on the gravity data by the bureau gravimetric international (Ahmad & Auwal, 2022).

### Methods

Various filtering techniques were applied on the residual magnetic/gravity field grid in order to aid interpretation. These filtering techniques were selected because they best delineate to support the research interest of the work. These techniques include:

#### First Vertical Derivative (FVD)

The first vertical derivative (high-pass filter) provides a more reliable outcome that is readily interpretable in the context of magnetic rock bodies (Jamaludin et al., 2021). The first derivative filtering is effective in enhancing the anomaly due to shallow sources by improving the spatial and structural resolution. Vertical derivative enhances shallow sources, suppressing deeper ones and gives a better resolution of closely spaced sources (Shehu et al., 2018).

This is done using the Laplace transformation expression below (Dalhatu et al., 2022)

$$\Delta 2f = 0 \quad (1)$$

Where  $\Delta 2f$  is the Laplace transformation which can be expressed in full as

$$\frac{\partial^2 f}{\partial z^2} = - \left[ \frac{\partial^2 f}{\partial x^2} + \frac{\partial^2 f}{\partial y^2} \right] \frac{\partial^2 f}{\partial x^2} \quad (2)$$

$\partial x$ ,  $\partial y$  and  $\partial z$  are differentials in x, y and z coordinates.

The nth vertical derivative can be computed using:

$$F \left[ \frac{\partial^2 f}{\partial z^n} \right] = K^n F(f) \quad (3)$$

### Analytical Signal (AS)

Analytic signal filter helps in reducing the sensitivity for the inclination of the geomagnetic field than the original TMI data and thus, provides means to analyze low latitude magnetic and gravity fields (Buckingham, 2015). Analytical signal maps capture the response of all anomalous bodies whether they are reversely magnetized or not. All the shape preserved on analytical signal maps is centered to one positive body and are not subject to the instability that occurs in transformations of magnetic fields from low magnetic latitude, thus able to define source positions regardless of any remnant magnetizations in sources (Milligan & Gunn, 1997).

The analytical signal  $A(x, z)$  gives the amplitude response of an anomaly, and is defined by Blakely (1995) as:

$$a(x, z) = \frac{\partial M}{\partial x} + i \frac{\partial M}{\partial z} \quad (4)$$

Where  $\frac{\partial M}{\partial x}$  and  $\frac{\partial M}{\partial z}$  are Hilbert transform pair.

The amplitude for the 2-D signal is given by

$$|A(X, Z)| = \sqrt{\left(\frac{\partial M}{\partial x}\right)^2 + \left(\frac{\partial M}{\partial z}\right)^2} \quad (5)$$

The 3-D analytical signal,  $A$ , of a potential field anomaly can be defined (Nabighian, 1984) as

$$A(x, y) = \left(\frac{\partial M}{\partial x}\right)X + \left(\frac{\partial M}{\partial y}\right)Y + \left(\frac{\partial M}{\partial z}\right)Z \quad (6)$$

Where  $M$  = Magnetic field

The analytical signal amplitude can now be calculated (Debeglia & Corpel, 1997) as

$$|A(X, Y)| = \sqrt{\left(\frac{\partial M}{\partial x}\right)^2 + \left(\frac{\partial M}{\partial y}\right)^2 + \left(\frac{\partial M}{\partial z}\right)^2} \quad (7)$$

### Source Parameter Imaging (SPI)

The important of Source Parameter Imaging (SPI) in magnetic and gravity survey analysis cannot be overemphasized. SPI is a technique based on the extension of complex analytic signal (AS) to estimate magnetic depths; it is also known as local wavenumber (Garba, 2021). Onwuemesi, (1997) to determine the depth of the agnetic sources, used this method. SPI produces accurate depth estimation similar to that of Euler deconvolution; however SPI has the advantage of producing a more complete set of coherent solution points and it is easier to use (Garba, 2021). The SPI computes source parameters from gridded magnetic data. Solution grids show the edge locations, depths, dips, and susceptibility contrasts. The depth estimation is independent of variables such as magnetic inclination, declination, dip, strike and/or remanent magnetization.

Thurston and Smith (1997) define the local wave number  $k$  (in radian per ground unit) for analytical signal to be

$$K = 2\pi f_o \quad (8)$$

And

$$f_o = \frac{1}{2\pi} \frac{\partial}{\partial x} \tan^{-1} \left[ \frac{\frac{\partial M(x,z)}{\partial z}}{\frac{\partial M(x,z)}{\partial x}} \right] \quad (9)$$

Where  $f_o$  is cycles/ground unit and  $K$  is the wave number in radian per ground unit.

$$K = \frac{\partial}{\partial x} \tan^{-1} \left[ \frac{\frac{\partial M(x,z)}{\partial z}}{\frac{\partial M(x,z)}{\partial x}} \right] \quad (10)$$

Nabighian (1972) gives the expression for the vertical and horizontal gradient of a sloping contact model as:

$$\frac{\partial M(x,z)}{\partial z} = \frac{2KFcsin\beta.xcos(21-\beta-90^\circ)-hsin(21-\beta-90^\circ)}{h^2+x^2} \quad (11)$$

And

$$\frac{\partial M(x,z)}{\partial x} = \frac{2KFcsin\beta.hcos(21-\beta-90^\circ)-xsin(21-\beta-90^\circ)}{h^2+x^2} \quad (12)$$

where  $K$  is the susceptibility contrast at the contact,  $F$  is the magnitude of the earth's magnetic field (the inducing field),  $c = 1 - \cos^2 \alpha$ ,  $\alpha$  is the angle between the positive x-



axis and magnetic north,  $i$  is the ambient-field inclination,  $\tan i = \sin i / \cos i$ ,  $\beta$  is the dip (measured from the positive x-axis),  $h$  is the depth to the top of the contact and all trigonometric arguments are in degrees. The coordinate system has been defined such that the origin of the profile line ( $x = 0$ ) is directly over the edge. Substituting equations 6 and 7 into 5 gives the wave number for a contact profile as:

$$K_{max} = \frac{1}{h} \quad (13)$$

And

$$\text{Depth } (h) = 1/K_{max} \quad (14)$$

Where  $K_{max}$  is wave number of the analytical signal  $h$  is the depth to the point of contact

Equation 26 is the basis for SPI method (Adetona & Abu, 2013). It utilizes the relationship between source depth and the local wave number of the observed field, which can be calculated for any point within a grid of data through horizontal and vertical gradients (Thurston & Smith, 1997).

#### Lineament Analysis

The lineaments from FVD was automatically traced out using the cet module available on oasis montaj software. The CET module was developed by the center for exploration targeting in the University of Western Australia to provide automated lineament detection of gridded data (CET, 2018). If a target is based on a set of intersection points ( $x_i, y_i$ ) from mapped lineaments:

$$X_c = \frac{1}{N} \sum_{i=1}^N x_i \quad (15)$$

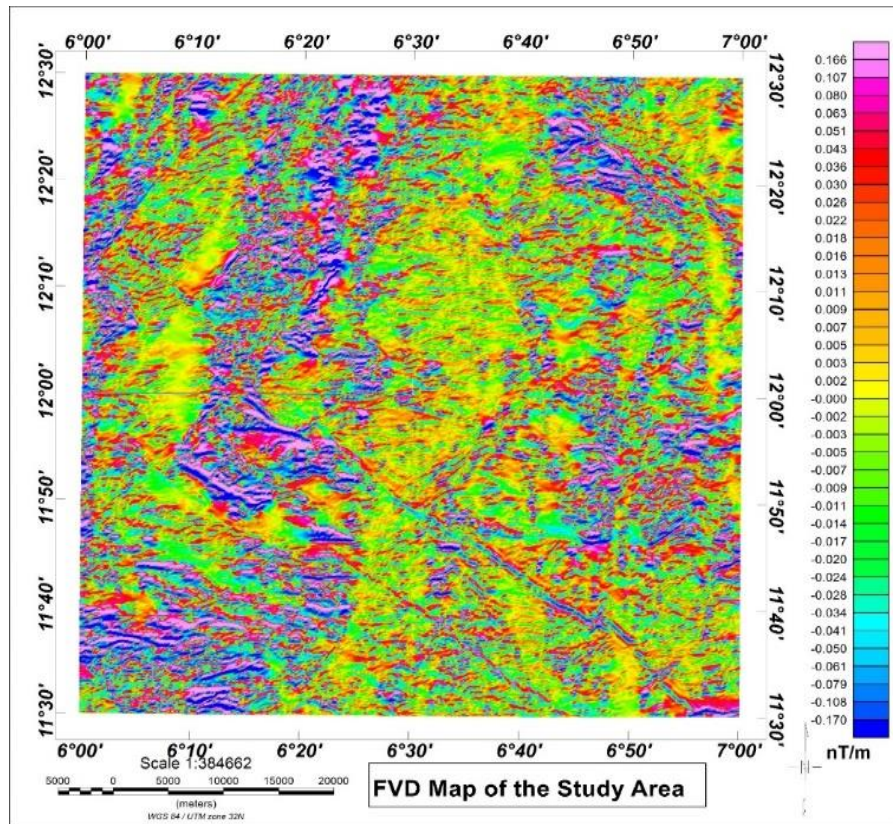
$$Y_c = \frac{1}{N} \sum_{i=1}^N y_i \quad (16)$$

Where  $X_c$  and  $Y_c$  are coordinates of the exploration target center

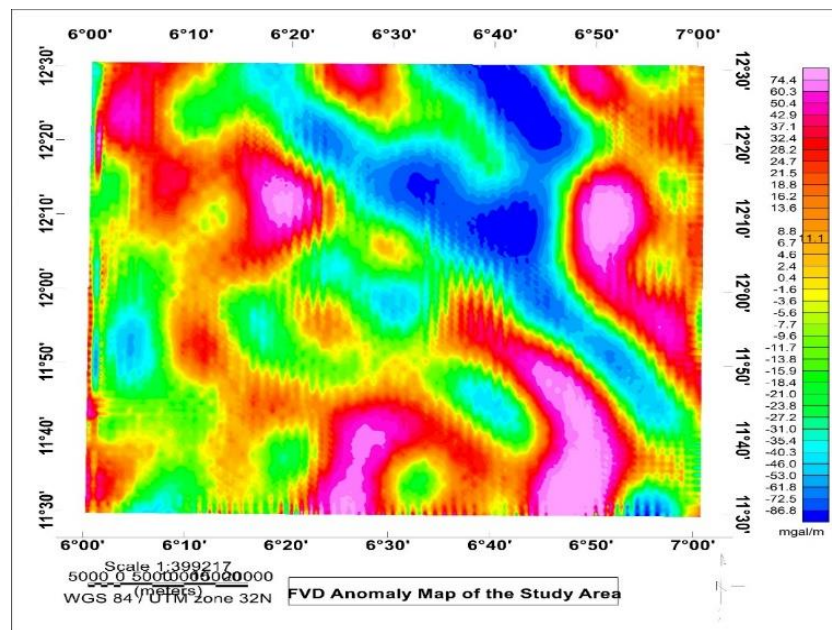
$N$  is the number of intersection points

## RESULTS AND DISCUSSION

Figure 3(a) represents the first vertical derivative map of magnetic data with the range of values from -0.170 nT/m to 0.166 nT/m. The first derivative filtering is effective in enhancing the anomaly due to shallow sources by improving the spatial and structural resolution. This map characterizes shallow anomalies (short wavelength) compared to its original TMI data. Thus, the low magnetic zone in the lower portion of the south corresponding to central part of Dan Gulbi in TMI map is now occupy by small-scale and dense high magnetic zones in the shallower section, as imaged on FVD data (figure 3a). It reveals the types of structures like lineament present in the study area. The major magnetic features (lineament) found on the study area aligned north northern to lower portion of the southwestern part (NN-SW), northwestern to the western (NW-W) as well as northeastern to southeastern (NE-SE) parts of the survey area. Since minerals are structurally controlled, the structures found in the study area might host the minerals present in the study area. To find out more about rock contact boundaries, it is necessary to do a gradient analysis process. Figure 3(b) is the gravity FVD (first vertical derivative) which aim to determine the location of the rock contact boundary in the study area. FVD has a value between -86.8 mgal/m to 74.4 mgal/m with the minimum value indicating the contact boundary of rock lithology in the study area. A system of N-SE trending negative anomalies, which are rimmed by positive anomalies is observed.



(a)



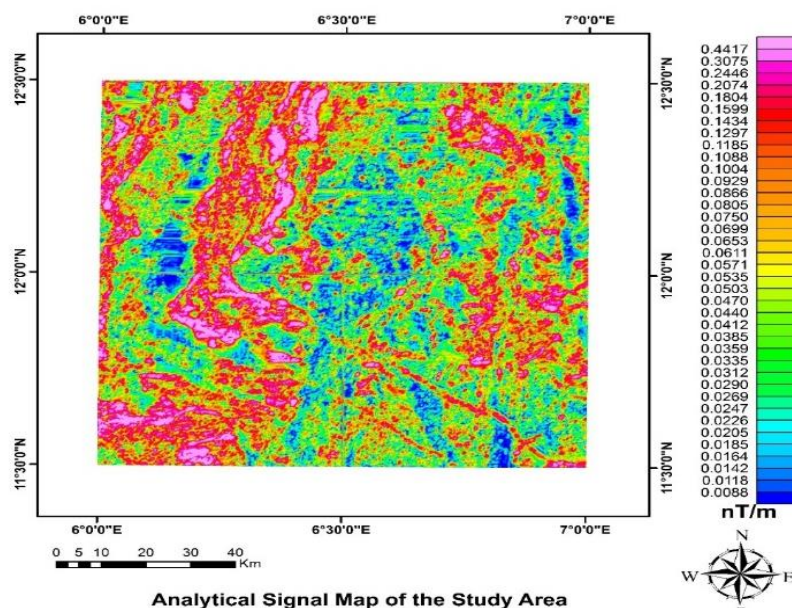
(b)

Figure 3: First Vertical Derivative Maps of (a) aeromagnetic data (b) aerogravity data

Figure 4(a) represent analytic signal map of magnetic data. It displays maximum amplitude directly over the edge of the magnetic source hence it is used to locate boundaries of magnetic bodies responsible for the anomalies. Two major regions can easily be observed figure 4(a); regions whose amplitude responses are high which are predominantly basement outcrops with varying degree of deformations and regions whose amplitude are low, which depicts regions with relatively good sedimentation. Areas with variable magnetic contrast were delineated with the amplitude of analytic signal varying from 0.0088 to 0.4417nT/m. High amplitude analytical signal values are observed in the remarkable trend of north northern to lower portion of the southwestern (NN-SW), northwestern to the western (NW-W) as well as

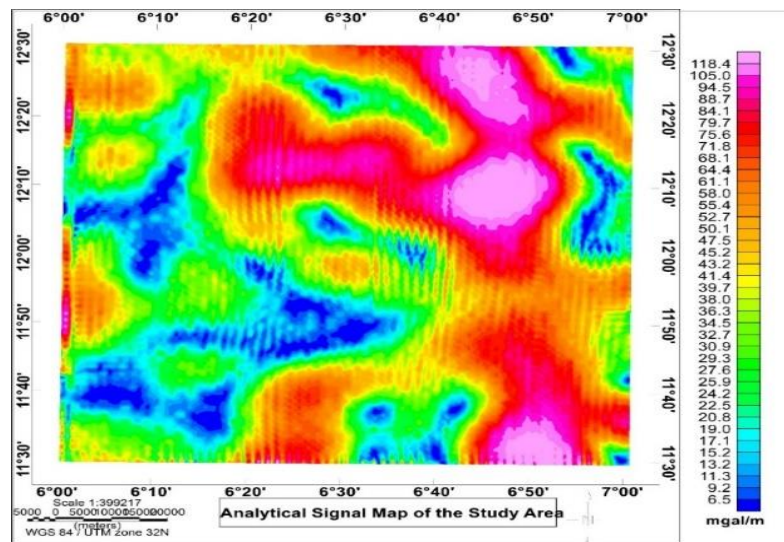
northeastern to southeastern (NE-SE) parts of the survey area. A structure suspected to be an intrusion (dike) is clearly aligned in NW- SE.

Gravity analytical signal (AS) map figure 4(b) with the range of amplitude values from low (6.5 mgal/m) to high (118.4mgal/m) delineates the presence of NN-SE oriented high amplitude anomalies bodies in the survey area, with local variations of geological bodies with low amplitude anomalies in the western and the central part of the study area. Two major regions can easily be observed from the map, regions whose amplitude responses are high which are predominantly basement outcrops with varying degree of deformations and regions whose amplitude are low, which depicts regions with relatively good sedimentation.



(a)





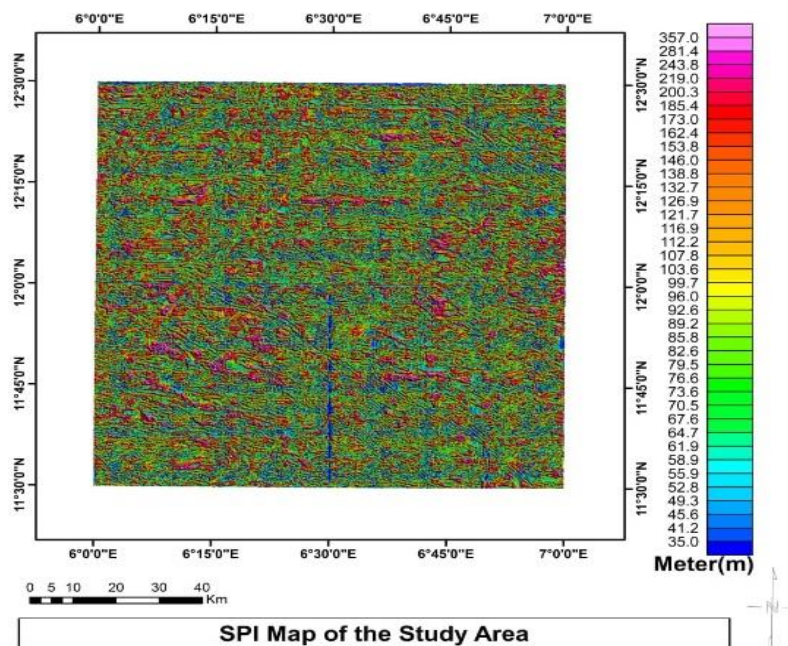
(b)

Figure 4: Analytical Signal Maps of (a) aeromagnetic data (b) aerogravity data

Figure 5(a) represents the source parameter imaging (SPI) map of the magnetic data. SPI technique was applied for structural features and estimate depth to the position causative bodies associate with mineralization potential. The depth range in this map is from 35.0m to 357.0m. SPI technique has helped in specifying the depth of the boundaries of causative bodies associated with minerals. The zones between 400m to 185.4m, 185.4m to 96.0m and 96.0m to 64.7m depth

corresponds to the regions of shear/faults/structural trends associated with solid mineral.

Figure 5(b) represents the source parameter imaging (SPI) map for gravity data. The depth range in this map is from 260.0m to 5192.5m. The zones between 5192.5m to 2394.04m, 2177.3m to 1222.3m and 1145.9m to 503.7m depth corresponds to the regions of shear/faults/structural trends associated with solid mineral.



(a)

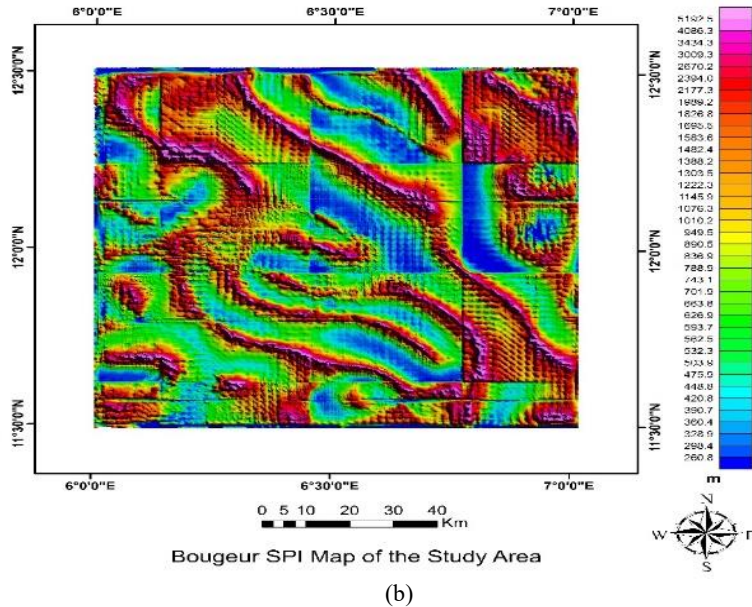
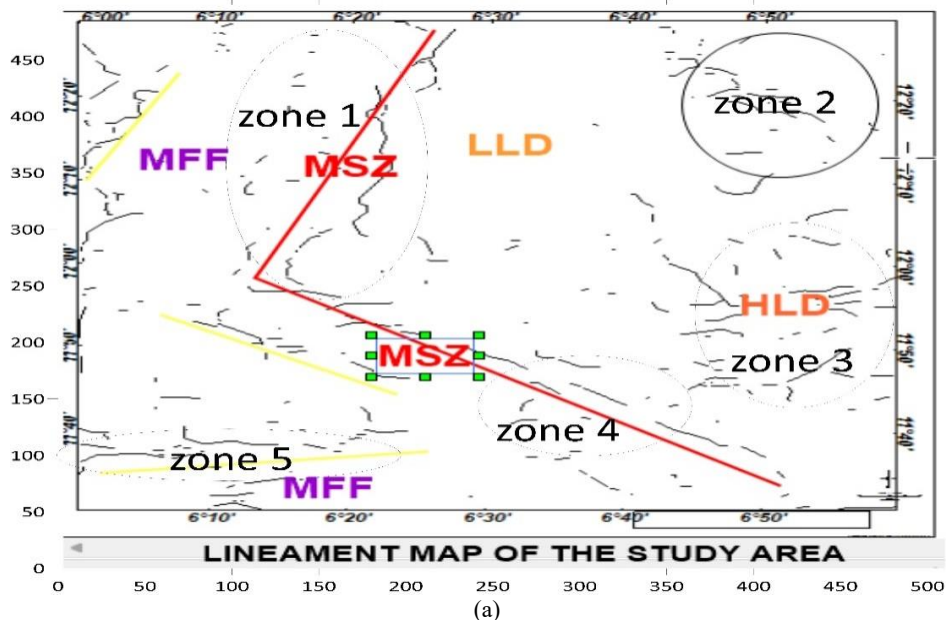


Figure 5: Source Parameter Imaging Maps of (a) aeromagnetic data (b) aerogravity data

The figure 6(a) below represents the magnetic lineaments map of the study area. The lineament map clearly shows the lineaments with a major trending of NN-SW and NW-SE with minor trending in all directions. These lineaments, depicting faults, fractures and contacts represents veins of possible mineralization. Different lineaments zones such as major faults and fractures (MFF), major shear zones (MSZ), high lineaments density (HLD) and low lineaments density (LLD) were all delineated in the lineament map of the study area.

The figure 6(b) is a gravity lineaments map of the study area. The map represents geological structures such as faults, joints,

lithological contacts, and shear zones from different rocks formation like medium to coarse-grained biotite, amphibolite schist, granite gneiss as well as sand and clay available in the study area. These geologic structures are important locations for potential minerals accumulation. In this figure, different lineament zones are highlighted in the map such as high lineaments density (HLD) trending NW-SE, low lineaments density (LLD) zones mostly oriented in the western part of the study area, major faults and fractures (MFF) trending E-W and minor faults and fractures zones (MFF) trending N-E.



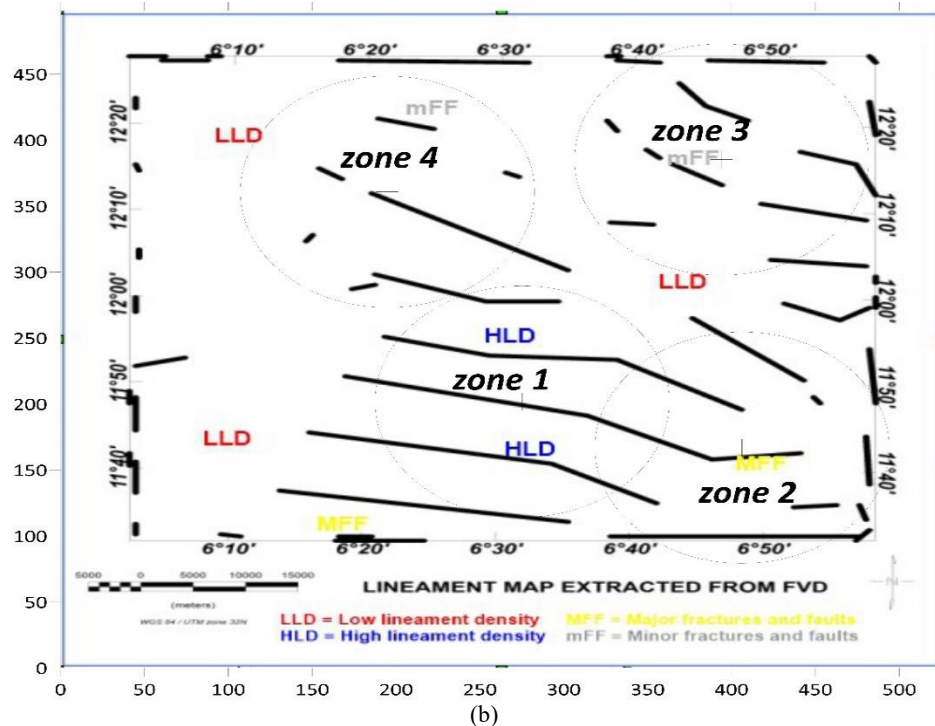


Figure 6: Magnetic Lineaments Maps of (a) aeromagnetic data (b) aerogravity data

### Structural Trend Analysis Results

The lineament maps (figures 6a and b) were used to determine the general structural trends in the studied area. The deduced structural maps (figures 7a and b) represent the fault system dissecting the area. The deduced fault planes of the different directions are grouped every 150 around the north for their length percentage 1% and represented by rose diagrams. The results of fault system deduced from both magnetic

lineaments map and gravity lineaments map were represented in the form of rose diagram as shown in (figures 7a and b). The results indicate that, most of the predominant directions are n 450e and s 1350w for aeromagnetic survey. The predominant trends for aerogravity survey according to figure 7b are NN 100 E, SS1900W. Some trends are also found in figures 7a and b as N600 E, S1450 W and S1000EE, N850 WW respectively.

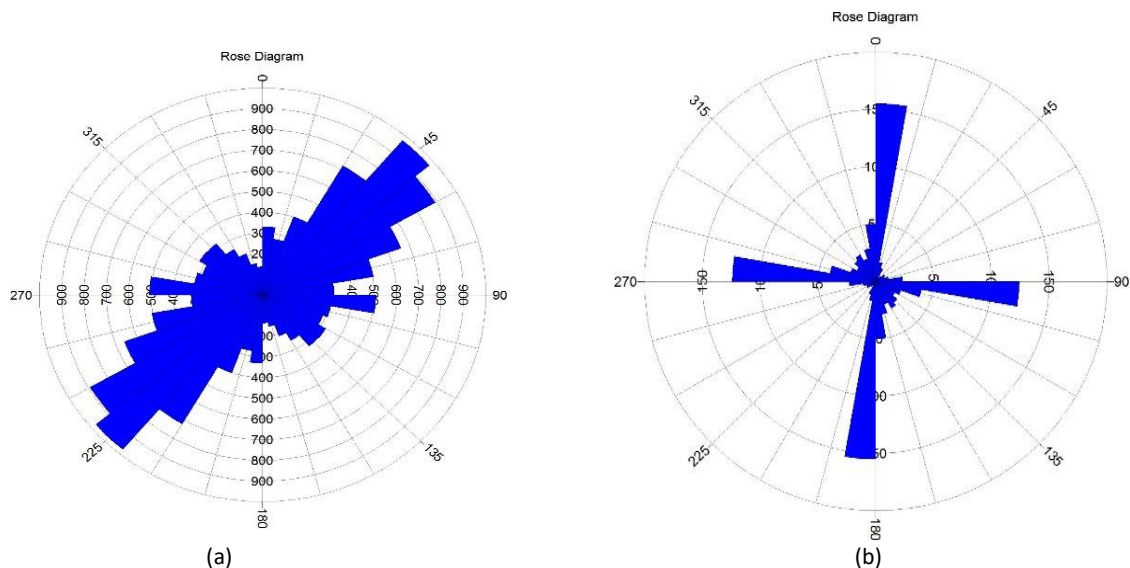


Figure 7: Rose Diagrams Deduced From (a) Aeromagnetic Lineaments Map. (b) Aero Gravity Lineaments Map



**Table 1: Location of Major Anomalous Zones**

Zones	Latitudes (0N)	Longitudes (0E)	Towns	Geological Settings
<b>Aeromagnetic</b>				
1	12.45	6.44	Lugga, Maru, Kukulai	Medium to coarse-grained biotite, migmatite augen gneiss.
	12.06	6.25		
2	12.46	6.73	Gidan Awala, Yantauri	Granite gneiss, Medium to coarse-grained biotite, granite and granite prophery, sand and clay.
	12.31	6.89		
3	11.98	6.94	Katanga,Chida, Magazu, Kanaure	Granite gneiss, sand and clay, migmatite augen gneiss, Medium to coarse-grained biotite.
	11.95	6.75		
4	11.77	6.59	Dutsin Kura, Ungwan Kane,	Migmatite augen gneiss, Amphibole schist amphibolite, Granite gneiss, sand and clay.
	11.88	6.46	Mazanya, Tudun Wada	
5	11.63	6.44	Dan Gulbi, Dan Kaina	Amphibole schist amphibolite, Medium to coarse-grained biotite Granite gneiss.
	11.64	6.23		
<b>Aerogravity</b>				
1	11.77	6.59	Dutsin Kura, Ungwan Kane,	Migmatite augen gneiss, Amphibole schist amphibolite, Granite gneiss, sand and clay.
	11.88	6.46	Mazanya, Tudun Wada	
2	11.64	6.78	Maraba Bawa, Kaura, Ungwan	Granite gneiss, sand and clay, migmatite augen gneiss, Medium to coarse-grained biotite.
	11.57	6.97	Hausa	
3	12.46	6.73	Gidan Awala, Yantauri	Granite gneiss, Medium to coarse-grained biotite, granite and granite prophery, sand and clay.
	12.31	6.89		
4	12.45	6.44	Lugga, Maru, Kukulai	Medium to coarse-grained biotite, migmatite augen gneiss.
	12.06	6.25		

The structural trends from magnetic lineaments map of southern part of Gusau and NE part of Tsafe are in agreement with Augie & Ridwan, (2021) who also obtained southern part of Gusau and NE part of Tsafe trending in his aeromagnetic studies of eastern part of Zamfara. Based on this study, predominant zones highlighted from both the aeromagnetic and aerogravity data analysis table 1 are zone 1, 2, 4 (MSZ and HLD) and zone 1, 3, 4 (MFF and HLD) respectively. The structures existed within the zones may extended to deep depths which can allow the hydrothermal solutions to pass through hosts rocks in the area forming hydrothermal alteration zones consociated with solid minerals (gold-bearing and quartz veins). Some mineral zones found in figure 6(a) are absent in figure 6(b) as zone 3 and 5 (MFF and HLD) in figure 6a are not found in figure 6b as LLD are recorded in the same location. Conversely, zone 2 in figure 6(b) (MFF) is not found in figure 6(a) as LLD are recorded in the same location. This confirmed that aeromagnetic anomaly map captures only magnetic response from the magnetic bodies within the subsurface of the study area while aerogravity anomaly map captures density contrast within the subsurface of the study area. The two lineaments maps show that the central part of Zamfara is an area with complex geologic structures. The result for depth estimation by Ibim et al., 2025 using two-dimensional (2D) radially averaged power spectrum technique revealed that the estimated average depth of the gravity source bodies is 2800 m for the deep and 280 m for the shallow source. However, the 2-D power spectrum diagram of the magnetic data. (Figure 6b) indicates, that the deeper source has an average depth of about 3800 m and the shallow is of about 800 m. It is noted that the average depth of the deeper magnetic data is more than gravity, as it somewhat directed to the basement surface as well as intra basement source. According to the depth estimation results, airborne gravity yields information for the deeper section whilst the aeromagnetic data facilitate information for the shallower section. As such, the potential mineral zones are

located several meters deep within the subsurface in the study area. Therefore, miners are urged to go deep in mineral deposits exploration within the specified locations in the study area.

## CONCLUSION

In this study, we found that the aeromagnetic anomalies maps capture magnetic response from the magnetic bodies, assume as the basement of central Zamfara while airborne gravity anomalies maps capture density contrast within the subsurface of the study area. The results from integration of the two potential methods has provided clear resolution and revealed the regions that might host mineralization potential. These areas have also revealed the alteration zones (faults, fractures/ or shears zones) that usually plays an important role in determining many minerals. The isolated potential mineral zones such as 12.450N, 11.880N 6.440E, 6.890E correspond to geologic setting with host rocks containing more of Fe-bearing minerals that form various silicates and oxide mineral species which may form during the formation of both intrusive and extrusive igneous rocks. The results from depth estimation technique reveals depth ranges from 35 m to 5000 m which has implications on feasibility such as cost-effectiveness of deep versus shallow mining. There is need for field validation like sampling, trenching, drilling to confirm the geophysical anomalies. Also integrated geochemical surveys, 3D inversion modeling and higher-resolution data acquisition to refine targets is also suggested. Delineating mineral zones can ease mining process and create a productive environment for business opportunities, boost the nation's economy and provide raw materials for industrial uses that might in turn reduce the level of unemployment thereby minimizing poverty.

## REFERENCES

Adagunodo, T.A., Sunmonu, L. A. & Adeniji, A.A. (2015). An Overview of Magnetic Method in Mineral Exploration

[J]. Journal of Global Ecology and Environment (2015), 3(1): 13 - 28.

Adekoya, J.A. (2003). Environmental Effect of Solid Minerals Mining, J. Phys. Sci. Kenya 625–640.

Adewumi, T. and Salako, K.A. (2018). Delineation of Mineral Potential Zone using High Resolution Aeromagnetic Data over Part of Nasarawa State, North Central, Nigeria, Egyptian Journal of Petroleum, <https://doi.org/10.1016/j.ejpe.2017.11.002>.

Adetona, A. A. and Abu, M. (2013). Estimating the Thickness of Sedimentation Within Lower Benue Basin and Upper Anambra Basin, Nigeria, Using Both Spectral Depth Determination and Source Parameter Imaging. Hindawi Publishing Corporation ISRN Geophysics. Pp, 1-10.

Augie, A.I. and Ologe, O. (2020). Analysis of Aeromagnetic Data for Coal Deposit Potential over Birnin Kebbi and its Environs Northwestern Nigeria, Nigerian Journal of Science and Environment, 18 (1): 145 – 153.

Augie, A.I. and Ridwan M.M. (2021). Delineation of Potential Mineral Zones from Aeromagnetic Data Over Eastern Part of Zamfara, Savanna Journal of Basic and Applied Sciences (June, 2021), 3(1): 60-66 P: ISSN 2695-2335 | E: ISSN 2705-3164.

Ahmad, A. and Alhasan, A. (2022). The Principle of Interpretation of Gravity Data Using Second Vertical Derivative Method. DOI: <http://dx.doi.org/10.5772/intechopen.100443>.

Buckingham, A. (2015) Magnetic and FTG Training Course (Day 3) Session 2; Fathom Geophysics: Kuala Lumpur, Malaysia, 2015; p. 25.

Blakely, R. J. (1995). Potential theory in gravity and magnetic applications. Cambridge University press. New York, 435p  
Centre for Exploration Targeting (CET) (2018). CET Grid Analysis. Retrieved 4th August, 2018 [www.cet.edu.au](http://www.cet.edu.au)

Dalhatu, B., Bonde D.S., Abbas M., Usman A., Liba A.M. (2022). Subsurface Investigation of Western Part of Zamfara Using Aeromagnetic Data. International Journal of Advances in Engineering and Management (IJAEM) Volume 4, Issue 1 Jan 2022, pp: 642-654 [www.ijaem.net](http://www.ijaem.net) ISSN:2395-5252

Debeglia, N. and Corpe, J. ((1997). Automatic 3-D Interpretation of Potential Field Data Using Analytic Signal Derivatives, Geophysics 62 (1) (1997) 87–96.

Fairhead, J.D. (2009). Potential Field Methods for Oil and Mineral Exploration GETECH/ Univ. of Leeds (2009), pp. 290.

Garba, M. E. (2021). “Aeromagnetic Study of Nickel Deposit Around Bakin Kogi in Jema’a Local Government Area of Kaduna State,” Thesis Work Submitted to the Department of Physics, Kaduna State University, Kaduna, 2021.

Indriyani, P.D., Rina D.I., Ode M.S., Arisuna P. (2023). Semarang Subsurface Model Using Airborne Gravity Data.

international Journal of Research and Review Vol. 10; Issue: 9; September 2023 Website: [www.ijrrjournal.com](http://www.ijrrjournal.com) Research Paper E-ISSN: 2349-9788; P-ISSN: 2454-2237 DOI: <https://doi.org/10.52403/ijshr.20230929>

Ibim, D.F., Amaechi, C. J., Nwinka, B. and Agogo, A.A. (2025). Gravity and Magnetic Techniques for the Delineation of Subterranean Structural Features of the Basement Complex, Imo River Basin, Southeastern Nigeria. International Journal of Applied Science and Engineering Volume 15, Number 2, 2025 Issn: 4461 – 4780

Jamaludin, S.N.F., Pubellier, M., Sautter, B. (2021). Shallow vs. Deep Subsurface Structures of Central Luconia Province, Offshore Malaysia Reveal by Aeromagnetic, Airborne Gravity and Seismic Data. Appl. Sci. 2021, 11, 5095. <https://doi.org/10.3390/app11115095>

Milligan, P. and Gunn, P. (1997). Enhancement and Presentation of Airborne Geophysical Data. AGSO J. Aust. Geol. Geophys. 1997. 17, 63–75.

Nabighian, M. N. (1972). The Analytic Signal of two-dimensional Magnetic Bodies With Polygonal Cross Section: Its Properties and Use for Automated Anomaly Interpretation. Geophysics. 37(2). pp. 507-517.

Onwuemesi, A. (1997). “One-dimensional Spectral Analysis of Aeromagnetic Anomalies and Curie Depth Isotherm in the Anambra Basin of Nig. Journ. Of Geodynamics”, vol. 23, no. 2, pp.95-107, 1997.

Priscillia, E., Abu, M., Abel, U.O., Adewumi T. (2021). Structural Exploration of Aeromagnetic Data over Part of Gwagwalada, Abuja for Potential Mineral Targets Using Derivatives Filters. Journal of Geological Research <http://ojs.bilpublishing.com/index.php/jgr-aARTICLE>

Sani, A.A. Augie, A.I. and Aku, M.O. (2019). Analysis of Gold Mineral Potentials in Anka Schist Belt North Western Nigeria using Aeromagnetic Data Interpretation, Journal of the Nigerian Association of Mathematical Physics, 52: 291-298.

Syafnur, A., Sunantyo T.A., Magister, D. Universitas, G., Mada, G. (2019). Potensi airborne gravity untuk studi sesar. Pros Semin Nas GEOTIK. 2019;392–9.

Shehu, S. J., Musa, O. A., Muhammad S., Abdulrahim, A. B. and Salihu B. S. (2018). A Reconnaissance Study to Delineate the Potential Mineral Zones Around the Schist Belt Areas of Kano State, Nigeria Using Airborne Magnetic Data. Journal Of Geology And Mining Research Vol. 11(2), pp. 14-21, March 2019 <https://doi.org/10.5897/JGMR2018.0307> Article Number: 657189460371 ISSN: 2006-9766 Copyright ©2019

Thurston, J. B. and Smith, R. S. (1997). Automatic Conversion of Magnetic Data to Depth, Dip and Susceptibility Contrast Using the SPITM Method. Geophysics, 62, pp, 807-813.



©2025 This is an Open Access article distributed under the terms of the Creative Commons Attribution 4.0 International license viewed via <https://creativecommons.org/licenses/by/4.0/> which permits unrestricted use, distribution, and reproduction in any medium, provided the original work is cited appropriately.